

# Dilepton production in $pp$ and $CC$ collisions with HADES

I.Fröhlich<sup>10</sup>, G.Agakishiev<sup>11</sup>, C.Agodí<sup>1</sup>, A.Balanda<sup>5</sup>, G.Bellia<sup>1,2</sup>, D.Belver<sup>19</sup>, A.Belyaev<sup>9</sup>, A.Blanco<sup>3</sup>, M.Böhmer<sup>15</sup>, J.L.Boyard<sup>17</sup>, P.Braun-Munzinger<sup>6</sup>, P.Cabanelas<sup>19</sup>, E.Castro<sup>19</sup>, S.Chernenko<sup>9</sup>, T.Christ<sup>15</sup>, M.Destefanis<sup>11</sup>, J.Díaz<sup>20</sup>, F.Dohrmann<sup>7</sup>, I.Durán<sup>19</sup>, T.Eberl<sup>15</sup>, L.Fabietti<sup>15</sup>, O.Fateev<sup>9</sup>, P.Finocchiaro<sup>1</sup>, P.J.R.Fonte<sup>3,4</sup>, J.Friese<sup>15</sup>, T.Galatyuk<sup>6</sup>, J.A.Garzón<sup>19</sup>, R.Gernhäuser<sup>15</sup>, C.Gilardi<sup>11</sup>, M.Golubeva<sup>14</sup>, D.González-Díaz<sup>6</sup>, E.Grosse<sup>7,8</sup>, F.Guber<sup>14</sup>, Ch.Hadjivasiliou<sup>16</sup>, M.Heilmann<sup>10</sup>, T.Hennino<sup>17</sup>, R.Holzmann<sup>6</sup>, A.Ierusalimov<sup>9</sup>, I.Iori<sup>12,13</sup>, A.Ivashkin<sup>14</sup>, M.Jurkovic<sup>15</sup>, B.Kämpfer<sup>7</sup>, K.Kanaki<sup>7</sup>, T.Karavicheva<sup>14</sup>, D.Kirschner<sup>11</sup>, I.Koenig<sup>6</sup>, W.Koenig<sup>6</sup>, B.W.Kolb<sup>6</sup>, R.Kotte<sup>7</sup>, F.Krizek<sup>18</sup>, R.Krücken<sup>15</sup>, A.Kugler<sup>18</sup>, W.Kühn<sup>11</sup>, A.Kurepin<sup>14</sup>, J.Lamas-Valverde<sup>19</sup>, S.Lang<sup>6</sup>, S.Lange<sup>6</sup>, L.Lopez<sup>3</sup>, A.Mangiarotti<sup>3</sup>, J.Marín<sup>19</sup>, J.Markert<sup>10</sup>, V.Metag<sup>11</sup>, B.Michalska<sup>5</sup>, D.Mishra<sup>11</sup>, E.Moriniere<sup>17</sup>, J.Mousa<sup>16</sup>, M.Münch<sup>6</sup>, C.Müntz<sup>10</sup>, L.Naumann<sup>7</sup>, R.Novotny<sup>11</sup>, J.Otwinowski<sup>5</sup>, Y.C.Pachmayer<sup>10</sup>, M.Palka<sup>5</sup>, V.Pechenov<sup>11</sup>, T.Pérez<sup>11</sup>, J.Pietraszko<sup>6</sup>, R.Pleskac<sup>18</sup>, V.Pospíšil<sup>18</sup>, W.Przygoda<sup>5</sup>, B.Ramstein<sup>17</sup>, A.Reshetin<sup>14</sup>, M.Roy-Stephan<sup>17</sup>, A.Rustamov<sup>6</sup>, A.Sadovsky<sup>7</sup>, B.Sailer<sup>15</sup>, P.Salabura<sup>5</sup>, A.Schmah<sup>6</sup>, P.Senger<sup>6</sup>, K.Shileev<sup>14</sup>, R.Simon<sup>6</sup>, S.Spataro<sup>1</sup>, B.Spruck<sup>11</sup>, H.Ströbele<sup>10</sup>, J.Stroth<sup>10,6</sup>, C.Sturm<sup>6</sup>, M.Sudol<sup>10,6</sup>, K.Teilab<sup>10</sup>, P.Tlusty<sup>18</sup>, M.Traxler<sup>6</sup>, R.Trebacz<sup>5</sup>, H.Tsertos<sup>16</sup>, I.Veretenkin<sup>14</sup>, V.Wagner<sup>18</sup>, H.Wen<sup>11</sup>, M.Wisniowski<sup>5</sup>, T.Wojcik<sup>5</sup>, J.Wüstenfeld<sup>7</sup>, Y.Zanevsky<sup>9</sup>, P.Zumbruch<sup>6</sup>

<sup>1</sup>) Istituto Nazionale di Fisica Nucleare - Laboratori Nazionali del Sud, 95125 Catania, Italy

<sup>2</sup>) Dipartimento di Fisica e Astronomia, Università di Catania, 95125, Catania, Italy

<sup>3</sup>) LIP-Laboratório de Instrumentação e Física Experimental de Partículas, Departamento de Física da Universidade de Coimbra, 3004-516 Coimbra, PORTUGAL.

- 4) ISEC Coimbra, Portugal
- 5) Smoluchowski Institute of Physics, Jagiellonian University of Cracow, 30059 Cracow, Poland
- 6) Gesellschaft für Schwerionenforschung mbH, 64291 Darmstadt, Germany
- 7) Institut für Kern- und Hadronenphysik, Forschungszentrum Rossendorf, PF 510119, 01314 Dresden, Germany
- 8) Technische Universität Dresden, 01062 Dresden, Germany
- 9) Joint Institute of Nuclear Research, 141980 Dubna, Russia
- 10) Institut für Kernphysik, Johann Wolfgang Goethe-Universität, 60486 Frankfurt, Germany
- 11) II.Physikalisches Institut, Justus Liebig Universität Giessen, 35392 Giessen, Germany
- 12) Istituto Nazionale di Fisica Nucleare, Sezione di Milano, 20133 Milano, Italy
- 13) Dipartimento di Fisica, Università di Milano, 20133 Milano, Italy
- 14) Institute for Nuclear Research, Russian Academy of Science, 117312 Moscow, Russia
- 15) Physik Department E12, Technische Universität München, 85748 Garching, Germany
- 16) Department of Physics, University of Cyprus, 1678 Nicosia, Cyprus
- 17) Institut de Physique Nucléaire d'Orsay, CNRS/IN2P3, 91406 Orsay Cedex, France
- 18) Nuclear Physics Institute, Academy of Sciences of Czech Republic, 25068 Rez, Czech Republic
- 19) Departamento de Física de Partículas. University of Santiago de Compostela. 15782 Santiago de Compostela, Spain
- 20) Instituto de Física Corpuscular, Universidad de Valencia-CSIC, 46100 Valencia, Spain

### Abstract

Dilepton production has been measured with HADES, the “High Acceptance DiElectron Spectrometer”. In  $pp$  collisions at 2.2 GeV kinetic beam energy, exclusive  $\eta$  production and the Dalitz decay  $\eta \rightarrow \gamma e^+ e^-$  has been reconstructed. The electromagnetic form factor is well in agreement with existing data. In addition, an inclusive  $e^+ e^-$  spectrum from the  $^{12}\text{C}+^{12}\text{C}$  reaction at 2 A GeV is presented and compared with a thermal model.

# 1 Introduction

One of the main open questions in QCD is the origin of the hadron masses. Beside the so-called Goldstone bosons like  $\pi$  and  $\eta$ , the typical mass scales of hadrons in the vacuum is in the order of GeV, whereas the current quark masses  $m_u, m_d$  are 5-15MeV. Based on this fundamental question it has been proposed that the mass of the hadrons is related to the spontaneous breaking of chiral symmetry, which should be partially restored at finite baryon and energy densities. In connection to this question, one of the topics in the modern hadron physics is how hadrons behave in strong interacting medium. This means that their properties - like mass and width - have to be measured inside either cold, dense or hot nuclear matter. In this context, vector mesons have been proposed as an ideal probe for such studies, since they decay via an intermediate virtual photon  $\gamma^*$  into dileptons ( $e^+e^-$  or  $\mu^+\mu^-$ ) which do not undergo strong interaction. Recently, the NA60 collaboration [1] has extracted the  $\rho - \omega$  line shape using the dimuon channel in In+In collisions at 158A GeV, which would correspond to a hot environment. These measurement indicates broadening of the line shape rather than a dropping of the mass.

However, for a complete understanding of the hadronic properties it is important to measure not only the hot, but also the dense region of the phase space. At beam energies of 1-2 A GeV, which corresponds to moderate densities (2-3  $\rho_0$ ), the production of mesons is dominated by multi-step excitations of a limited number resonances and their subsequent decays, like  $\Delta^{+,0} \rightarrow N\pi^0 \rightarrow N\gamma e^+e^-$  ( $\pi$ -Dalitz),  $\Delta \rightarrow Ne^+e^-$  ( $\Delta$ -Dalitz),  $N^*(1535) \rightarrow N\eta \rightarrow N\gamma e^+e^-$  ( $\eta$ -Dalitz) and the decay of virtual resonances in  $N(\omega, \rho)$ . Here, most of the production mechanisms are at or even below threshold, which means that mesons are more likely produced in the dense phase of the fireball evolution.

The result of such experiments is usually a dilepton invariant mass spectrum containing all these sources (dilepton-cocktail). Before a conclusion on the properties of  $\rho$  and  $\omega$  can be drawn, the contribution of Dalitz decays have to be subtracted.

## 2 Properties of the virtual photon

For a more detailed view, it is very helpful to know that a virtual photon (decaying into 2 stable particles) has 6 degrees of freedom: First, its invariant mass  $M_{\gamma^*}^{inv}$ . Moreover the momentum  $P_{\gamma^*}^X$ , the polar  $\theta_{\gamma^*}^X$  and the azimuthal angle  $\phi_{\gamma^*}^X$  of the

virtual photon in the rest frame of the source  $X$ . Angles are defined with respect to the production plane and momentum transfer. Finally, the 2 decay angles of the photon into the dilepton pair, which are usually described with the helicity angle  $\theta_e^{ee}$  (which is the angle of one lepton in the dilepton rest frame, with respect to the direction of the photon), and the Treiman-Yang angle  $\phi_e^{ee}$  (the orientation of the decay plane around the photon direction). Since a detector has a finite acceptance as a function of total phase space, for an interpretation of the invariant mass spectrum  $M_{\gamma^*}^{inv}$  the additional distribution functions have to be known. For the pseudoscalar mesons, these are well under control: For a spin-less state, no alignment information can be carried from the production mechanism to the decay, so  $\theta_{\gamma^*}^X$ ,  $\phi_{\gamma^*}^X$  and  $\phi_e^{ee}$  are isotropic. The helicity angle is proposed to be  $1 + \cos^2 \theta_e^{ee}$  [2]. For a given mass of  $\gamma^*$  its momentum is fixed by the mass of the meson. The only degree of freedom is the mass spectrum, which is based on a well-know electromagnetic form factor [3]. In total, the pseudoscalar mesons have no uncertainty and are a good choice for a detector performance test.

This is very different for the  $\Delta$  Dalitz decay, because for particles carrying spin, production and decay do not factorize. In addition, the form factor as well as the branching ratio are based on calculations [4] and the helicity angle has quite some uncertainties [2]. For the direct decay of vector mesons, the helicity angle has to be isotropic, but the Treiman-Yang angle could contain higher order contributions. Moreover, the  $\omega \rightarrow \pi^0 e^+ e^-$  transition form factor cannot be consistently described within the vector meson dominance model. This shows, that it is not only important to measure the dilepton production in heavy ion collision, but collect also information of the individual sources to avoid systematic errors based on the detector acceptance. This is one of the goals of the HADES detector (GSI, Darmstadt). Therefore, its program spans from  $pp$ ,  $\pi p$  to  $\pi A$  and  $AA$  collisions. First data has been taken in  $CC$  collisions at 1 and 2AGeV,  $ArK + Cl$  collisions at 1.78AGeV, and  $pp$  at 1.25 and 2.2GeV.

A more detailed view of the detector can be found in [5, 6]. Shortly, HADES is a magnetic spectrometer, consisting of up to 4 mini drift chambers (MDC) with an toroidal magnetic field. Particle identification is done based on time-of-flight measurements. In addition, a Ring Imaging Cherenkov detector (RICH) and an electromagnetic Pre-Shower detector adds lepton identification features.

### 3 The $pp \rightarrow pp\eta$ reaction at 2.2GeV

In January 2004 the first  $pp$  run has been carried out at a kinetic beam energy of 2.2GeV, in order to study the performance of the detector using the exclusive reaction  $pp \rightarrow pp\eta$  which has been measured by the DISTO collaboration before [7] at kinetic beam energies of 2.15, 2.5 and 2.85GeV. Since the decays  $\eta \rightarrow \pi^+\pi^-\pi^0$  [8] and  $\eta \rightarrow \gamma e^+e^-$  [3] are known, it served as a calibration reaction and first test if HADES is able to measure electromagnetic form factors. The analysis techniques are described in detail elsewhere [9]. Basically, for both reaction types kinematical constraints were used to identify the missing particle  $\pi^0$  or  $\gamma$ , respectively. In addition, a kinematic refit reduced the background.

#### 3.1 The hadronic decay $\eta \rightarrow \pi^+\pi^-\pi^0$

By using a selection on  $\cos(\theta_\eta^{CM})$  and fitting the corresponding  $pp$  missing-mass spectrum, the angular distribution of the  $\eta$  meson emission has been evaluated. The acceptance correction has been done using a full Monte-Carlo simulation with generated events of  $pp \rightarrow pM \rightarrow pp\eta$  where the shape  $M \rightarrow p\eta$  was taken from [7]. Only the alignment of the  $pp\eta$  plane has been left according to phase space. Together with the fact that the beam axis has rotational symmetry, only two angles are left for the alignment of the  $pp\eta$  plane, which are almost independent, thus allowing to compare directly 1-dimensional angular distributions. After the full analysis chain, generated and accepted events have been divided as a function of  $\cos(\theta_\eta^{CM})$ . Results are shown in Fig. 1 together with the found distribution by DISTO with an anisotropy coefficient ( $2^{nd}$ -order Legendre polynomial) of  $c_2 = -0.32 \pm 0.10$ . A fit on the data gives  $c_2 = -0.14 \pm 0.09$ , which tends more to an isotropic  $\eta$  production, but is still consistent within error bars with the previous result, showing that the hadron efficiency is understood as a function of phase space.

#### 3.2 The Dalitz decay $\eta \rightarrow \gamma e^+e^-$

Similar methods have been used for the  $\eta$  Dalitz decay. In addition, a selection on the opening angle of larger  $4^\circ$  was used to reject contributions by  $\eta \rightarrow \gamma\gamma$  and a subsequent conversion in the detector material. The invariant mass was used as the observable which was corrected for acceptance and efficiency. Again, by fitting the  $pp$  missing-mass spectrum for each invariant mass slice, the yield has been extracted. For the acceptance correction, the known production angles have

been fixed in the simulation, and the known  $\eta$  decay properties have been used as described in Sec. 2. Fig. 2 shows the corrected invariant mass spectrum [10] together with functions using the QED as well as vector meson dominance model (VDM) form factor [3] which have been normalized to the number of  $\eta$ 's found by experiment. In addition, each data point has been corrected in position according to the strong slope of the models. It can be seen that HADES is not sensitive to distinguish these 2 models, but at least agrees to the predictions within the given errors. This demonstrates that the efficiency is understood as a function of the invariant mass, which is the main important observable in the heavy ion data. In addition, the ratio between the 2  $\eta$  decay channels ( $R = \frac{N_{\eta \rightarrow \pi^+ \pi^- \pi^0}}{N_{\eta \rightarrow \gamma e^+ e^-}}$ ) have been calculated for a full-cocktail simulation and the data. The result is  $R_{exp} = 15.3 \pm 1.8_{stat}$  and  $R_{sim} = 15.6 \pm 0.9_{stat}$ , a nice agreement confirming that the lepton response of the HADES spectrometer is well understood [9].

## 4 Results on C+C at 2AGeV

The first result on dilepton production in C+C collisions at a kinetic beam energy of 2AGeV is ready for publication [11]. Details of the basic analysis steps can also be found in [12]. Basically, leptons are identified via the RICH detector and reconstructed using the MDCs. An opening angle of the pair of  $9^\circ$  has been applied to remove background from conversion. Finally, the combinatorial background (i.e. pairs mixed from different sources) has been removed by the like-sign method. For events with masses ( $M_{ee}^{inv} > 0.5 GeV/c^2$ ) the combinatorial background has been evaluated using the event-mixing technique.

In contrast to exclusive reactions, in heavy ion reactions only the final dilepton cocktail can be shown, without any selection on the different sources. As explained above, the virtual photon properties might vary, thus the extrapolation to  $4\pi$  is difficult, since 6 independent variables should be taken into account. While the integration over these variables cannot be done, a different method has been chosen. First, a single track efficiency as a function of  $p_e^{lab}, \theta_e^{lab}, \phi_e^{lab}$  has been extracted by simulation and applied to the data. This reduces the acceptance to a binary value. In order to compare the efficiency corrected data to any model, an acceptance filter has been developed [13]. Fig. 3 shows the invariant mass spectrum after all analysis steps. Absolute normalization has been done by a measurement of the charged pions, whose mean is the number of  $\pi^0$  in a isospin-symmetric reaction.

In order to make a statement for the contribution of the vector mesons, a sim-

ulation has been made based on a simple thermal model [14] and filtered with the detector acceptance. The resulting curves are shown also in Fig. 3. The solid line contains the  $\pi$  and  $\eta$  Dalitz decays with the decay properties as described above and the known production cross sections and distribution from TAPS [15]. It can be seen, that the  $\pi^0$  region is well described, however already in the  $\eta$  region model and data disagree. It is clear that additional sources are needed.

For a more complete view,  $\Delta$  production has been added by  $\pi^0$  scaling and the vector meson production by  $m_T$  scaling [16]. However, still a factor of around 2 remains in the mass region of  $0.2\text{GeV}/c^2 < M_{ee}^{inv} < 0.7\text{GeV}/c^2$ , where the  $\Delta$  decay is part of the contribution, as well as the low mass tail of the  $\rho$  meson. It has to be clarified if this enhancement is due to a different  $\Delta$  yield and/or decay properties, or modified vector meson shapes in the dense medium. This means that the HADES data has to be compared to advanced model calculations[17, 18, 19], which on the other hand needs as much constraints as possible extracted by elementary collisions.

## 5 Summary and Outlook

In summary, results for dilepton production obtained with HADES in elementary as well as heavy ion collisions have been presented. While the analysis of the beam times described in this work is almost finished, the  $CC$  collision at 1AGeV is under analysis. In addition, the  $pp$  run at 1.25GeV (below the  $\eta$  threshold) dedicated to  $\Delta$  production has collected in spring 2006 promising statistics. Systematic studies using elementary reactions will be continued, which is of particular importance for the interpretation of heavy ion inclusive mass spectra.

The collaboration gratefully acknowledges the support by BMBF grants 06TM970I, 06GI146I, 06F-140, and 06DR120 (Germany), by GSI (TM-FR1,GI/ME3,OF/STR), by grants GA CR 202/00/1668 and GA AS CR IAA1048304 (Czech Republic), by grant KBN 1P03B05629 (Poland), by INFN (Italy), by CNRS/IN2P3 (France), by grants MCYT FPA2000-2041-C02-02 and XUGA PGID T02PXIC20605PN (Spain), by grant UCY-10.3.11.12 (Cyprus), by INTAS grant 03-51-3208 and EU contract RII3-CT-2004-506078.

## References

- [1] R. Arnaldi et al., Phys.Rev.Lett. **96**, (2006) 162302.

- [2] E.L. Bratkovskaya, O.V. Teryaev and V.D. Toneev, Phys.Lett. **B348**, (1995) 283.
- [3] L.G. Landsberg Phys.Repts. **128**, (1985) 301.
- [4] C. Ernst et al., Phys.Rev.C **58**, (1998) 447.
- [5] R. Schicker et al., Nucl.Instr.Meth **A380**, (1996) 586.
- [6] A. Agakichiev et al., Nucl.Instr.Meth, to be published.
- [7] F. Balestra et al., Phys. Rev. **C69** (2004) 064003.
- [8] C. Amsler et al., Phys. Lett. **B 346** (1995) 203.
- [9] S. Spataro for the HADES collaboration, proceedings of the Meson 2006, Int.J.Mod.Phys, to be published.
- [10] B. Spruck, PhD thesis, University of Gießen.
- [11] A. Agakichiev et al., Phys.Rev.Lett, submitted, nucl-ex/0608031
- [12] Th. Eberl for the HADES collaboration, Eur.Phys.J, to be published.
- [13] R. Holzmann, unpublished. (requests to r.holzmann@gsi.de)
- [14] M.A. Kagarlis, GSI Report 200-03 (2000), unpublished.
- [15] R. Auerbeck et al., Z. Phys. A **359** (1997) 65.
- [16] E.L. Bratkovskaya, W. Cassing and U. Mosel, Phys.Lett. **B424**, (1998) 244.
- [17] W. Cassing and E.L. Bratkovskaya, Phys.Rept. **308**, (1999) 65.
- [18] K. Shekhter et al, Phys.Rev. **C68**, (2003) 014904. M.D. Cozma, C. Fuchs, E. Santini, A. Faessler, Phys.Lett. **B640**, (2006) 150.
- [19] D. Schumacher, S. Vogel and M. Bleicher, nucl-th/0608041.

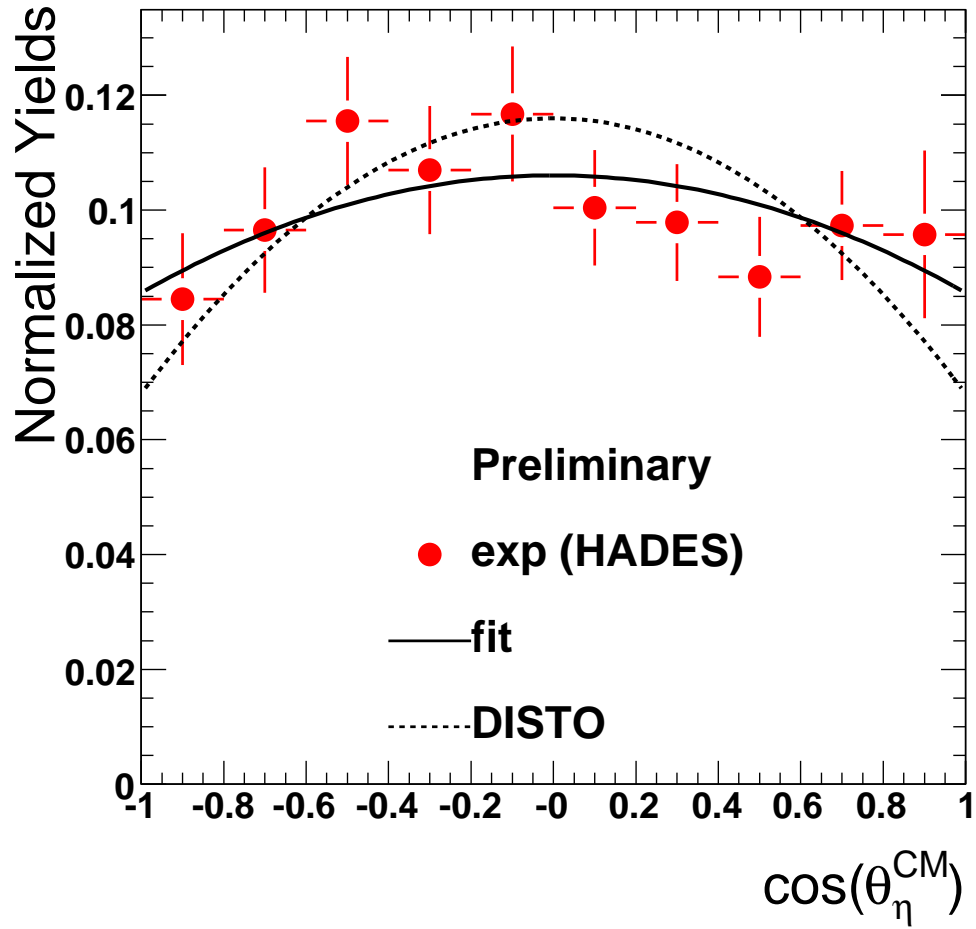


Figure 1: Distribution of the  $\eta$  polar production angle in the center of mass frame (statistical errors only). The plot is corrected for acceptance. The solid line represents a fit to the data, whereas the dashed lines shows a parametrization for the existing [7] in the same beam energy regime.

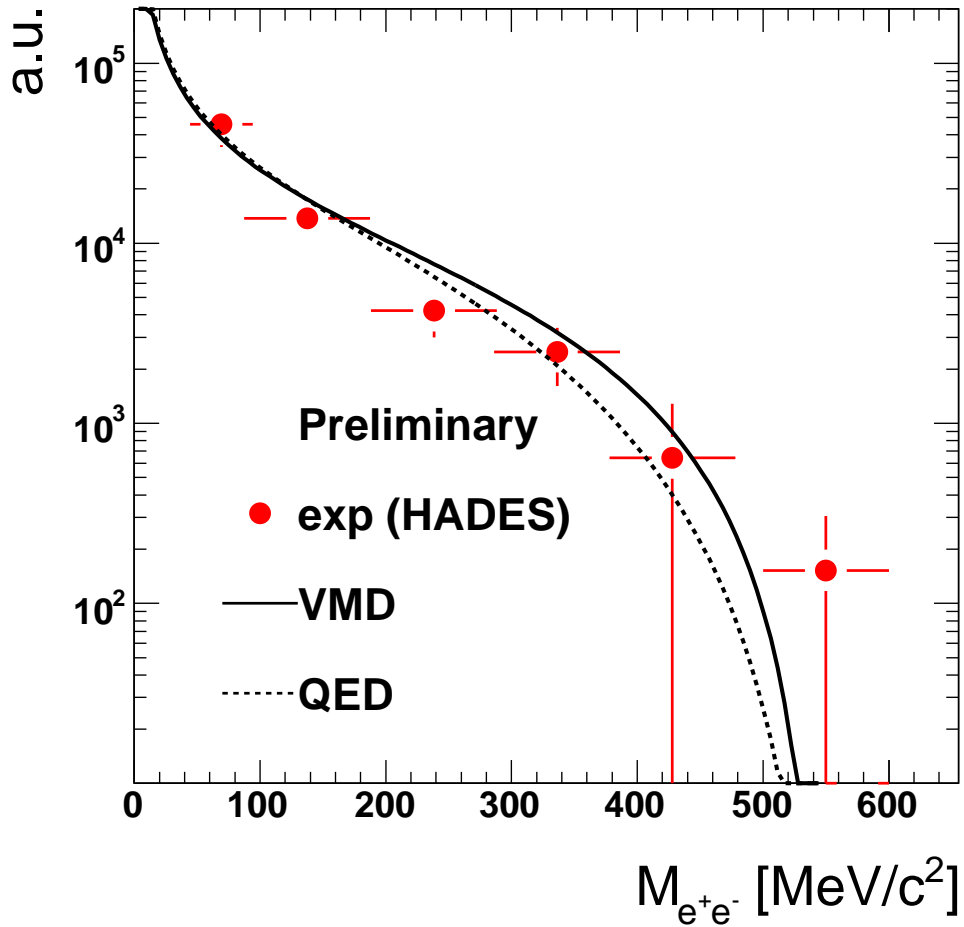


Figure 2: Invariant mass distribution  $M_{ee}^{inv}$  for the decay  $\eta \rightarrow \gamma e^+ e^-$  [10] (statistical errors only). The dashed line is showing the prediction for a simple QED factor, while the solid one represents the full VDM calculation [3].

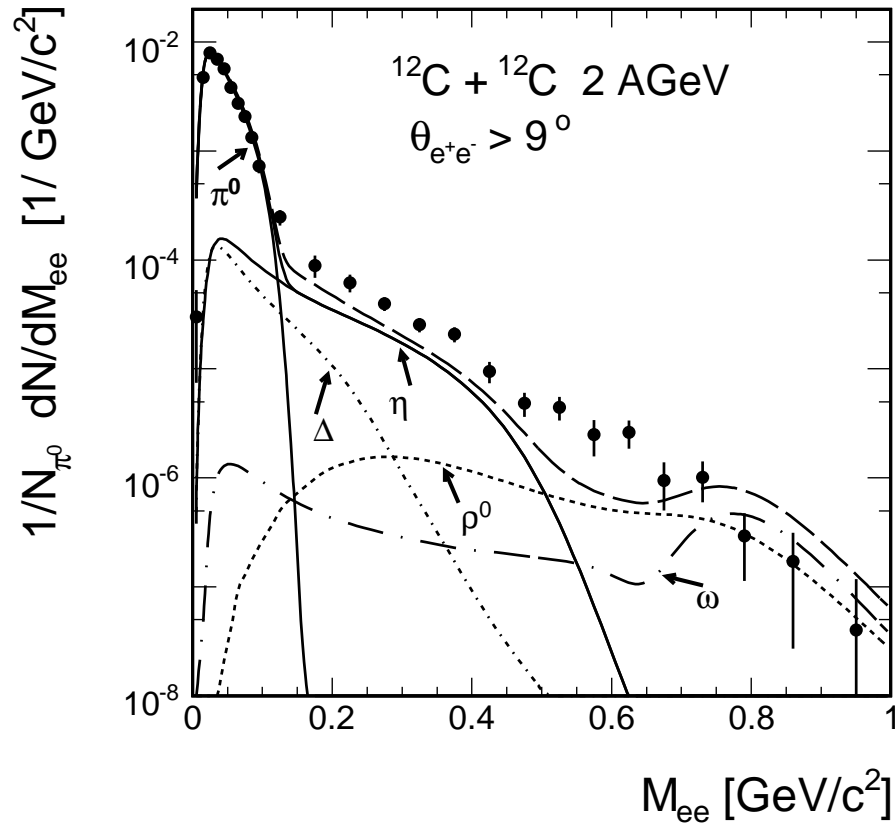


Figure 3: Invariant mass distribution  $M_{ee}^{inv}$  for  $CC$  at  $2A\text{GeV}$  [12]. The data points contain statistical error only. The lines are a thermal model simulation as described in the text